ORIGINAL ARTICLE

Brain and Behavior
Open Access WILEY

Managing electromyogram contamination in scalp recordings: An approach identifying reliable beta and gamma EEG features of psychoses or other disorders

Kenneth J. Pope[1,2] | Trent W. Lewis[1,2] | Sean P. Fitzgibbon[3] | Azin S. Janani[1,4] | Tyler S. Grummett[1,2,5] | Patricia A. H. Williams[1,6] | Malcolm Battersby[7,8] | Tarun Bastiampillai[7,8] | Emma M. Whitham[7,9] | John O. Willoughby[7,9]

[1]College of Science and Engineering, Flinders University, Adelaide, South Australia, Australia

[2]Medical Device Research Institute, Flinders University, Adelaide, South Australia, Australia

[3]Wellcome Centre for Integrative Neuroimaging, FMRIB, Nuffield Department of Clinical Neurosciences, University of Oxford, Oxford, UK

[4]School of Information Technology and Electrical Engineering, The University of Queensland, Brisbane, Queensland, Australia

[5]Adelaide Institute for Sleep Health, Flinders University, Adelaide, South Australia, Australia

[6]Flinders Digital Health Research Centre, Flinders University, Adelaide, South Australia, Australia

[7]College of Medicine and Public Health, Flinders University, Adelaide, South Australia, Australia

[8]Department of Psychiatry, Flinders Medical Centre, Adelaide, South Australia, Australia

[9]Department of Neurology, Flinders Medical Centre, Adelaide, South Australia, Australia

Correspondence
John O. Willoughby, Department of Neurology, College of Medicine and Public Health, Flinders University, GPO Box 2100, Adelaide SA 5001, Australia.
Email: John.Willoughby@flinders.edu.au

Abstract

Objective: In publications on the electroencephalographic (EEG) features of psychoses and other disorders, various methods are utilized to diminish electromyogram (EMG) contamination. The extent of residual EMG contamination using these methods has not been recognized. Here, we seek to emphasize the extent of residual EMG contamination of EEG.

Methods: We compared scalp electrical recordings after applying different EMG-pruning methods with recordings of EMG-free data from 6 fully paralyzed healthy subjects. We calculated the ratio of the power of pruned, normal scalp electrical recordings in the six subjects, to the power of unpruned recordings in the same subjects when paralyzed. We produced "contamination graphs" for different pruning methods.

Results: EMG contamination exceeds EEG signals progressively more as frequencies exceed 25 Hz and with distance from the vertex. In contrast, Laplacian signals are spared in central scalp areas, even to 100 Hz.

Conclusion: Given probable EMG contamination of EEG in psychiatric and other studies, few findings on beta- or gamma-frequency power can be relied upon. Based on the effectiveness of current methods of EEG de-contamination, investigators should be able to reanalyze recorded data, reevaluate conclusions from high-frequency EEG data, and be aware of limitations of the methods.

KEYWORDS
EEG, EMG contamination, psychoses, spectral analysis

1 | INTRODUCTION

The etiology of the psychoses likely involves a complex combination of genetic, neurodevelopmental, neurodegenerative, and environmental factors and there are reasons to propose that high-frequency electroencephalographic (EEG) rhythms might be informative. For example, in addition to the positive and negative symptoms of schizophrenia, other symptoms include cognitive decline, and impaired cognitive processes such as working memory, which are based on synchronized neural oscillations, particularly in the beta/gamma (25–40+ Hz) frequency ranges (McCutcheon et al., 2020; Uhlhaas & Singer, 2013). These rhythms are generated by phasic activity in GABAergic interneurons that input onto fast-firing pyramidal neurons, and thus produce high-frequency beta/gamma oscillations (Deutsch et al., 2010; Reynolds et al., 2004). Patients with schizophrenia have fewer pyramidal cell dendritic spines (as shown in auditory and dorsolateral prefrontal cortex) (Gonzalez-Burgos et al., 2015) that impair excitatory input to pyramidal cells and, thereby, reduce pyramidal cell activation, including onto GABAergic interneurons. The consequence is reduced recurrent inhibitory regulation of pyramidal cells (Coyle et al., 2012; Rujescu et al., 2006). Also potentially relevant to a GABAergic abnormality in schizophrenia is clozapine's unique mechanism of action: compared to other antipsychotics for treatment-resistant schizophrenia, clozapine may have specific GABAergic properties (Nair et al., 2020). Evidence for beta/gamma EEG dysfunction in schizophrenia also comes from studies showing reduced auditory steady-state responses (Brenner et al., 2009; O'Donnell et al., 2013; Onitsuka et al., 2013), so that aberrant beta/gamma activity likely underlies both the cognitive and negative symptoms of schizophrenia (Lewis et al., 2012).

There has been extensive investigation of beta/gamma activity in the standard resting electroencephalogram (EEG) in psychoses, but recent reviews have been unable to identify consistent beta or gamma EEG findings (Lavoie et al., 2019; Newson & Thiagarajan, 2018; Reilly et al., 2018). However, the problem of electromyogram (EMG) contamination plagues resting EEG beta/gamma in normal scalp recordings and could explain the absence of robust findings in resting EEG studies. We have examined this question by comparing EEG recorded before (EMG-contaminated) and after total neuromuscular paralysis (EMG-free) in healthy volunteers.

EMG contamination exceeds EEG power five- to 200-fold in the 50–100 Hz range over much of the scalp, relatively sparing only the central scalp area and frequencies below 20 Hz (Pope et al., 2009; Whitham et al., 2007, 2008).

While various approaches are used to reduce EMG contamination (EMG "pruning" methods) in psychiatric studies (Reilly et al., 2018), testing the effectiveness of various methods against EMG-free data reveals that none of the methods fully eliminate EMG contamination of resting EEG (Dharmaprani et al., 2016; Fitzgibbon et al., 2013, 2015, 2016; Janani et al., 2017, 2020; Janani, Grummett, Bakhshayesh, et al., 2018; Janani, Grummett, Lewis, et al., 2018). Thus, inconsistencies or negative findings may be due to biological variability in EMG contamination at different scalp locations and at different frequencies

in different patient groups. Even when methods such as independent component analysis (ICA) are used, an inadequate number of electrodes sometimes prevent their reliable application (Janani, Grummett, Bakhshayesh, et al., 2018). While calculated-Laplacian estimations of current source density (CSD) also addresses EMG contamination for the central scalp (Fitzgibbon et al., 2013, 2015), this method has infrequently been applied to continuous EEG.

To assist investigators in determining which published findings are likely to be based on valid, EMG-uncontaminated data, in this paper we show the possible extent of EMG contamination of continuous EEG using a range of available EMG-pruning methods, from the minimally processed through to the best method we are aware of. Currently, the latter is canonical correlation analysis (CCA) used with a support vector machine (SVM) to classify components, hence "pruned-CCA-SVM" (Janani et al., 2020). In this paper, we compare spectral power of pruned EEG data to EMG-free data and present the estimated residual contribution of EMG contamination in "contamination graphs." These estimates in healthy subjects should be helpful in evaluating previously published work in psychoses and are salutary indicators of the severity of the problem. They may provide motivation for researchers to reanalyze their recorded data or reevaluate their conclusions on high-frequency EEG data recorded away from the central scalp.

2 | METHODS

2.1 | Subjects

We applied a range of EMG-pruning methods to scalp electrical recordings from six healthy subjects and calculated the extent to which spectral power of the processed scalp electrical recording exceeded EMG-free EEG from the same subjects when paralyzed. The experiment was undertaken in volunteer EEG Unit staff and other colleagues, after approval by the Flinders Clinical Research Ethics Committee. Subjects were seated within the Faraday cage in a semi-recumbent posture and had a laryngeal mask in situ to enable artificial ventilation after paralysis. Cisatracurium (20 mg, intravenously) was used for paralysis and glycopyrrolate (0.2–0.4 mg) was used to diminish oral secretions. Paralysis lasted approximately an hour.

These data have been utilized in papers on the EMG contamination problem published by our group over the last 13 years, initially with two and, ultimately, with six subjects (Fitzgibbon et al., 2013, 2015, 2016; Janani et al., 2017, 2020; Janani, Grummett, Bakhshayesh, et al., 2018; Pope et al., 2009; Whitham et al., 2007, 2008).

2.2 | Data

EEG was recorded using a 128-channel system (Compumedics Pty Ltd., Melbourne, Australia) while the subjects undertook various tasks, including resting-eyes-closed, before and again after total

neuromuscular blockade (Whitham et al., 2007, 2008). (Note: the subjects were semi-recumbent with their head resting on the recliner chair, so the extent of EMG contamination of electrodes close to cervical muscles would be less than expected in studies with the head unsupported.)

2.3 | Data processing

First, we applied the EEGLab detrend algorithm from the SIFT toolbox (Delorme et al., 2011) to remove low-frequency noise, and the Clean-RawData algorithm to remove channels with a low correlation ($r < .85$) relative to the other channels. The resulting data are what we will refer to as "EMG-contaminated" data. We then applied several EMG-pruning methods.

2.3.1 | Independent component analysis

This identifies common signals (independent components) contributing to subsets of electrodes (Delorme & Makeig, 2004). These components may correspond, for example, to EEG, eye movements, blinks, electrocardiogram, or muscle contraction, and the contaminants are selectively discarded. Electrode recordings can then be calculated without contributions from contaminating components. We used ICA Infomax from EEGLab and also used spectral slope to assist in identifying neural components (Cardoso, 1997). Spectral slope refers to the shape of the power spectrum of each component and assists in classifying a component as brain or muscle origin. EMG has more sustained power between 7 and 75 Hz (Goncharova et al., 2003), so has a "flatter" slope than EEG.

2.3.2 | CCA or CCA-SVM with spectral slope

This method utilizes CCA to obtain components and their spectral slopes (De Clercq et al., 2006) and uses SVM to identify brain or non-brain components, including electrical noise (Dharmaprani et al., 2016; Fitzgibbon et al., 2016; Janani, Grummett, Bakhshayesh, et al., 2018; Janani et al., 2020).

2.3.3 | Calculated Laplacian

The Laplacian transform provides a different measure of brain activity than EEG (Fitzgibbon et al., 2013; Kayser & Tenke, 2015). It calculates the amount of current emerging perpendicularly from the brain surface, that is, scalp current density. For electrodes where there is no underlying cranial or scalp muscle, Laplacian reveals brain activity with minimal contaminating signal from muscle. We calculated the surface Laplacian using the spline interpolation method of Perrin and colleagues (Perrin et al., 1989).

2.4 | Estimates of residual EMG contamination

In each participant, we calculated ratios of processed (unparalyzed) spectral power to the EMG-free (paralyzed) spectral power for commonly used EEG bands: delta (1–4 Hz), theta (4–8 Hz), alpha (8–13 Hz), beta (13–30 Hz), gamma1 (30–50 Hz), and gamma2 (50–100 Hz), although we excluded 48–52 and 98–100 Hz power due to line noise and its first harmonic.

We plotted the means and standard errors of ratios for the six participants, yielding "contamination graphs": plots indicating the power of contaminants relative to the power of brain signals, at each recorded channel and for each frequency band. Additionally, the ratios of spectral power were also calculated from the Laplacians of the processed and EMG-free time series. This allows a direct comparison of the effectiveness of including a Laplacian calculation in artifact reduction. Calculations were always made using all valid 115-channel data.

2.5 | Review of recent studies in psychoses

Using the contamination graphs (Figures 1 and 3) as a guide, we assessed papers that described analyses of resting beta and gamma EEG in psychiatric populations published since the reviews of Newson and Thiagarajan (2018) and Reilly et al. (2018). We excluded studies using time-locked signal averaging, intracranial, magnetoencephalographic, or nonhuman recordings, or those where no beta/gamma claims were made.

3 | RESULTS

Figures show contamination graphs at the 21 channels of the 10–20 montage. Graphs showing all channels can be found in Appendix Figure A1. The graphs include EMG-contaminated data, and data pruned by three algorithms: pruned-CCA-EEGLab, pruned-ICA-EEGLab, and pruned-CCA-SVM. Figures 2 and 4 include a Laplacian processing step. Figures 1 and 2 show frequency bands, whereas Figures 3 and 4 use a continuous frequency axis.

3.1 | Beta and gamma

Contamination graphs for EMG-contaminated EEG (Figure 1) show EMG to be prominent in gamma bands (>30 Hz) across the entire scalp. With Laplacian processing, however, there was limited or no EMG contamination at central scalp sites (Figure 2). In the EEG, contamination also occurs to a lesser extent in the beta band, around twofold, and more if recordings are away from the central scalp (Figures 1 and 2).

CCA-EEGLab-processed EEG remains contaminated almost as much as unprocessed EEG (Figure 1). For Laplacians, CCA-EEGLab provides a slight further improvement in contamination of the peripheral (EMG-contaminated) electrodes (Figure 2).
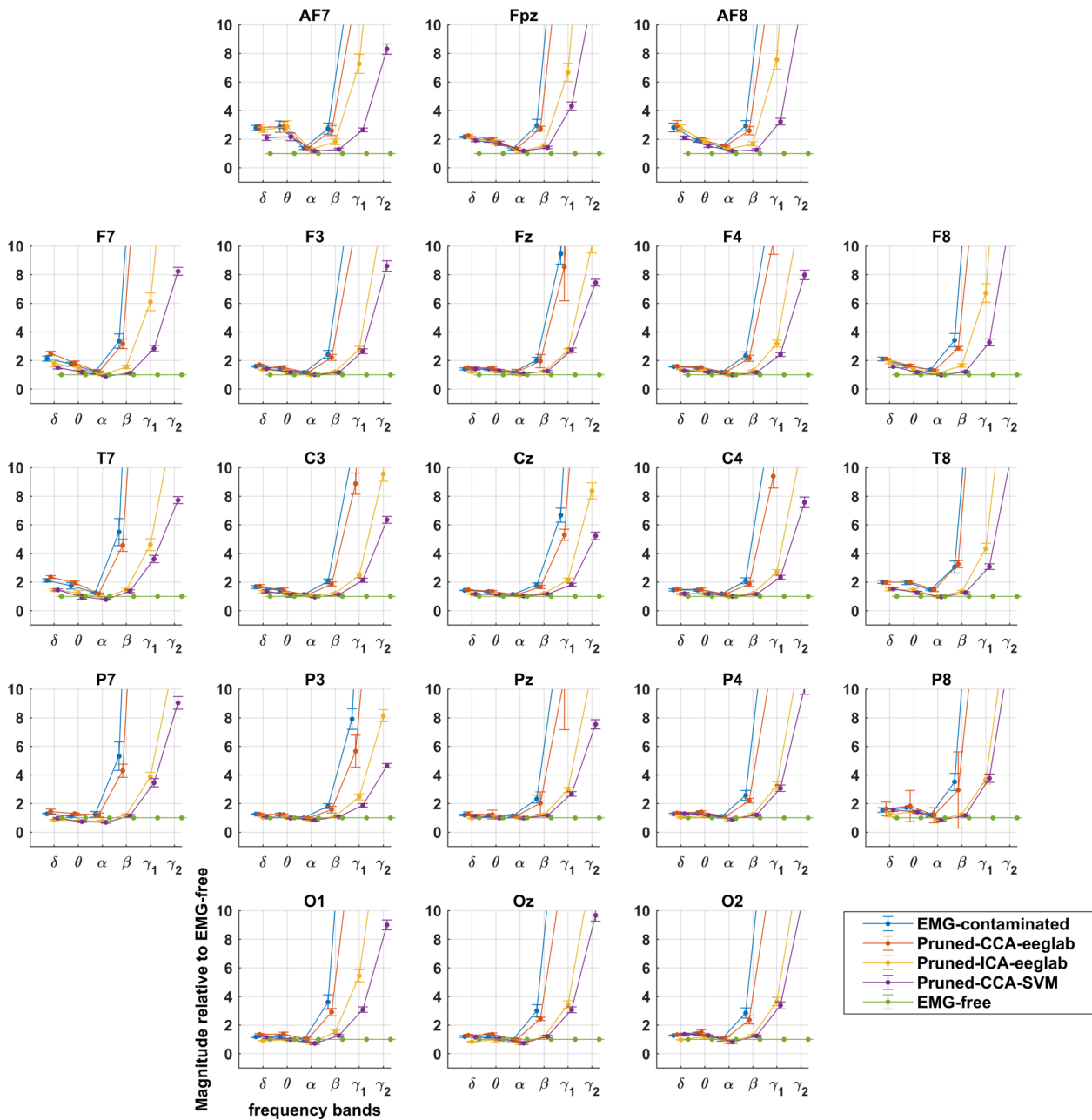
FIGURE 1 Montage showing extent of EMG contamination of EEG relative to EMG-free recording with different pruning methods. Divergence from EMG-free is prominent in gamma bands and increased with increasing distance from the central scalp at Cz. Delta and theta bands show small increases, while alpha bands are reduced during paralysis (see also Figure 3).

ICA-EEGLab achieves effective pruning of EMG in beta EEG activity in nearly all leads; however, gamma1 and 2 EEG remain heavily contaminated (Figure 1). ICA-EEGLab sometimes markedly improves Laplacians in the few electrodes that are contaminated in the very lateral or posterior scalp (Figure 2).

CCA-SVM achieves good pruning in beta EEG activity, even in lateral leads. Gamma EEG activity, however, remains severely contaminated (Figure 1). In contrast, Laplacian transforms of CCA-SVM data almost eliminate EMG contamination over the entire scalp (Figure 2). There is slightly less beta and gamma power for CCA-SVM than EMG-free, possibly related to reduced contamination by electrical line noise identified by the SVM (see Section 4).

Thus, for EEG, no pruning method achieves beta and gamma band power equivalent to EMG-free across the scalp. In a large central scalp area, and in contrast to EEG, Laplacian data have very low levels of EMG contamination across the full spectrum to 100 Hz.

3.2 | Delta through alpha

In delta, theta, and alpha frequencies, contamination graphs (see spectra in Figures 3 and 4) reveal little variation relative to EMG-free power, but slight increases or reductions from EMG-free can be seen. The increases (delta and theta) have a similar distribution to the
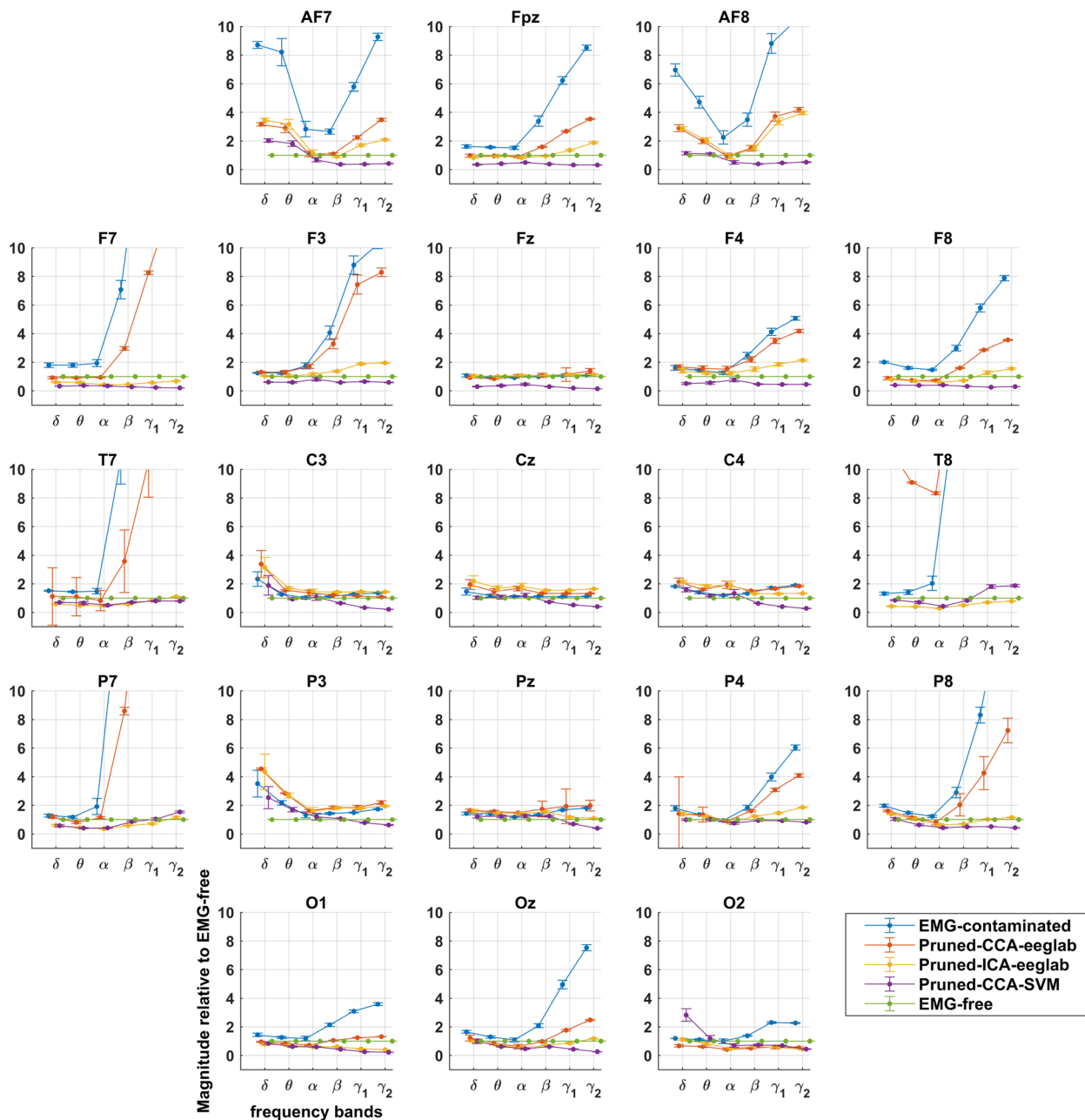
FIGURE 2   Montage showing extent of EMG contamination of Laplacians relative to EMG-free recording with different pruning methods. Divergence from EMG-free is prominent in gamma bands and increased with increasing distance from the central scalp at Cz. Delta and theta bands also show increases, while alpha bands are reduced during paralysis (see also Figure 4).

distribution of the most serious contamination due to muscle, pointing to ongoing subtle muscle contractions in the unparalyzed subjects (see Section 4). Alpha reductions have a posterior distribution, unlike the distribution of severe EMG contamination, so that an alternative explanation likely applies, possibly related to different mental states between the resting-unparalyzed and resting-paralyzed recordings (see Section 4).

The frequencies at which divergence appears are around the beta/gamma boundary (25–35 Hz), displayed best in Figures 3 and 4. Again, the Laplacian results reveal minimal broad-spectrum contamination in central leads, and high levels of contamination very peripherally, except when pruning methods have been applied.

3.3 | Pruning methods

Here, we use the extent of residual contamination as a guide to the relative effectiveness of the pruning methods: thus, lower levels of contamination indicate better effectiveness.

Of the methods we display here, pruned-CCA-SVM performs best. Pruned-ICA-EEGLAB is next most effective, but diverges away from pruned-CCA-SVM, most prominently where EMG activity is normally prominent, in very anterior and lateral leads (viz., F7, AF7, Fpz, AF8, and F8).

Although we have displayed 21 channel montages, contamination graphs from more peripheral locations exhibited even more EMG
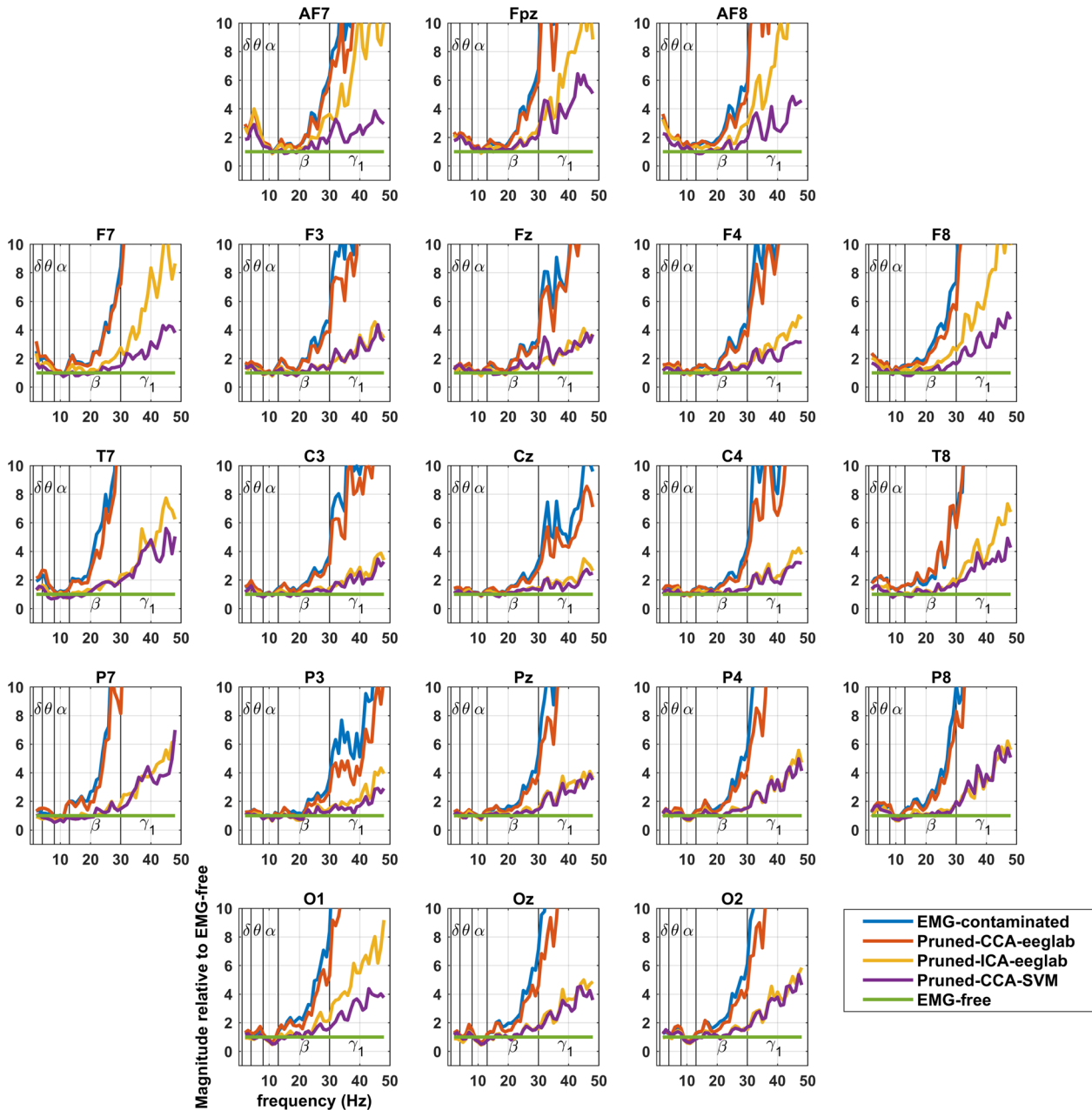
FIGURE 3 Montage showing extent of EMG contamination of EEG relative to EMG-free to better display the frequency at which spectral power increases above EMG-free. Delta and theta frequencies also show increases, while alpha frequencies are reduced posteriorly during paralysis.

contamination. Appendix A1 shows contamination graphs for all 115 electrodes using Laplacians and the three pruning methods, to supplement the information in Figure 2.

3.4 | Review of recent literature of beta/gamma EEG in psychoses

There were no publications whose results were exclusively drawn from adequately pruned data from central scalp areas below 30 Hz.

4 | DISCUSSION

It is clear that EMG contamination continues to confound the analysis of high frequencies in the resting EEG, even when studies utilize careful artifact editing of recordings. The contamination graphs illustrate the difficulties that investigators will have in interpreting their own data, a situation we previously experienced (Fitzgibbon et al., 2004; Willoughby, Fitzgibbon, Pope, Mackenzie, Medvedev, et al., 2003; Willoughby, Fitzgibbon, Pope, Mackenzie, Davey, et al., 2003). While increases in gamma or beta EEG power could theoretically be
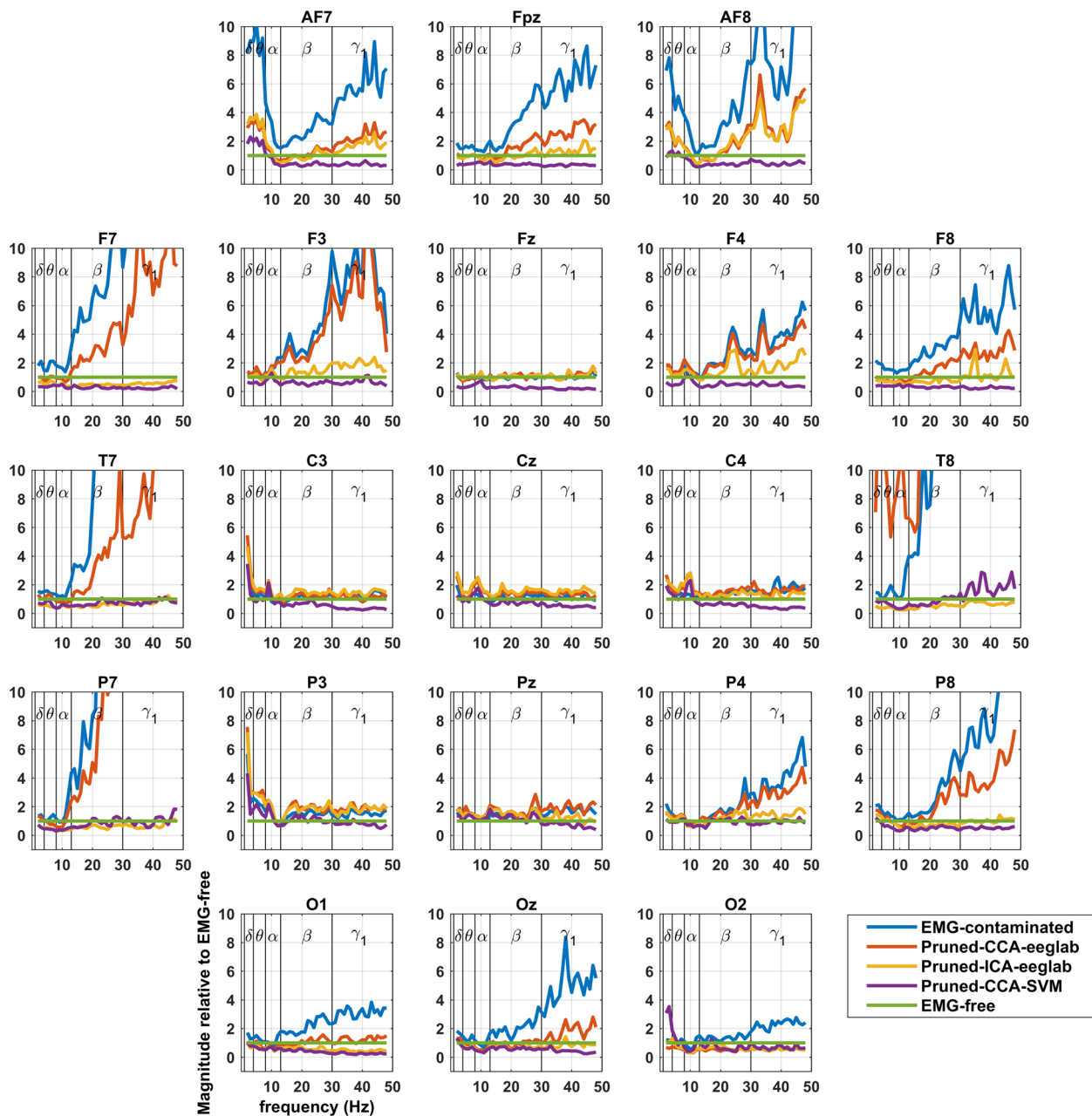
FIGURE 4 Montage showing extent of EMG contamination of Laplacians relative to EMG-free to better display the frequency at which spectral power increases above EMG-free

measured above baseline EMG power, attributing a signal increase to a brain effect, rather than to a small change in the five- to 40-fold baseline muscle power, is an insecure way to discover EEG correlates of psychoses or any other disorder.

4.1 | Considering the EEG spectrum

The frequency at which power diverges from EMG-free EEG (best shown in Figure 3) is approximately 20 Hz in unprocessed recordings and, after processing, approximately 40 Hz in much of the central scalp with both CCA-SVM and ICA-EEGLab. The useful range of EEG frequencies is roughly doubled by the use of these pruning methods.

As previously published, the most effective of the pruning methods is CCA-SVM: it permits the interpretation of EEG spectra at slightly higher frequencies and in a slightly larger area than ICA-EEGLab (Janani et al., 2020). The slight reduction in beta and gamma relative power with CCA-SVM Laplacians may be related to CCA-SVM identifying noise components in the line voltage (Janani et al., 2020).

4.2 | Considering Laplacian data

Applying the Laplacian transform to derive CSD is clearly effective in avoiding EMG contamination in central scalp areas, though not peripherally when close to underlying muscles (Figures 2 and 4). At central

sites, its effectiveness across the spectrum is a clear advantage over all other methods (compare Figures 3 and 4) and, furthermore, in the sub-50 Hz range, it extends the area of effectiveness to a larger central area than that provided by CCA-SVM EEG.

The advantage of the Laplacian method for central scalp sites provides motivation for analysis of Laplacian recordings as a routine in disease conditions. In this study, Laplacians were calculated from 120 channel EEG, covering the entire scalp, and enabled EMG-free measurement of brain activity in central scalp areas. Clearly, there would be a distinct advantage in recording Laplacians where this can be done reliably. The development of a tripolar concentric ring electrode, which records the Laplacian directly in hardware, offers this prospect (Koka & Besio, 2007) and is something we plan to evaluate.

4.3 | Considering other bands

The small increases in relative power in delta and theta bands pre-paralysis are consistent with delta and theta components being normal components of the resting EMG—as noted by Goncharova et al. (2003). Alternatively, it is also possible that total paralysis causes its own "brain state" characterized by reduced delta and theta activity. However, the low frequency increases in power occur with a similar distribution to the most serious contamination due to EMG (see Figures 1 and 3), consistent with EMG activity and/or with imperceptible motion artifact, for example, from other physiological activity such as respiration (Uriguen & Garcia-Zapirain, 2015). The small reductions in alpha power, relative to the paralyzed state, have an occipital distribution and could possibly be attributed to enhanced mental alertness prior to being paralyzed and then, after paralysis was fully established, increased relaxation, both physical and mental.

Since EMG contamination confounds studies of resting EEG, how can investigators safely proceed? We suggest general rules would be as follows: start with at least 64-channel recordings; always prune resting EEG recordings, the best methods being Infomax EEGLAB and CCA-SVM (Janani et al., 2020); after pruning, apply Laplacian transforms to provide reliable data in central scalp areas by reference to Appendix Figure A1. When confined to using EEG, if EEG power is increased at frequencies above 25 Hz, suspect EMG contamination, and if the finding becomes increasingly obvious away from the central cranium, assume the finding is EMG-confounded.

Currently, the diagnosis of psychoses (schizophrenia, schizoaffective, and bipolar disorder) is based only on clinical interview, collateral history, and behavioral observation. There is no valid diagnostic test for psychoses like those that exist for other conditions (cancer, heart disease, etc.) and delays in initial diagnosis impede efforts to initiate treatment early and reduce the duration of untreated psychosis. Reducing the duration of untreated psychosis can reduce long-term morbidity and improve quality of life. At present, the possibility of an abnormality in the resting EEG remains to be properly explored, specifically using Laplacian measurement. Such a finding would greatly assist diagnosis and likely further contribute to the current findings from The Bipolar and Schizophrenia Network for Intermediate Phe-

notypes (Tamminga et al., 2017) that is trying to develop a biomarker framework to categorize these conditions. It would further motivate drug discovery with a focus on GABAergic compounds for the treatment of psychoses: beta/gamma EEG abnormalities point specifically to GABAergic therapeutic interventions that might improve cognition and the negative symptoms of schizophrenia, which do not respond to current dopamine D2 antagonists. The question of beta/gamma resting EEG changes in psychoses requires further attention to aid in possible etiological understanding, aiding earlier diagnosis, guiding prognosis, and possibly monitoring response to pharmacological treatment.

5 | CONCLUSION

Estimates of EMG contamination of scalp EEG in the range 1–100 Hz reveal that no method of EMG pruning adequately decontaminates EEG data in the analysis of beta and gamma frequencies. Laplacian/CSD methods combined with pruning methods can provide EMG-free measures in central scalp areas. Based on the contamination graphs we have provided, it should be possible for EEG laboratories with signals-processing expertise to reevaluate existing high-density EEG recordings using the methods we tested. For laboratories without signal-processing expertise, reliable conclusions should be possible using original data in safe frequencies and scalp locations.

CONFLICT OF INTEREST
The authors declare no conflict of interest.

DATA AVAILABILITY STATEMENT
The data will be provided on reasonable request.

PEER REVIEW
The peer review history for this article is available at: https://publons.com/publon/10.1002/brb3.2721.

ORCID
John O. Willoughby https://orcid.org/0000-0003-0457-7117

REFERENCES
Uhlhaas, P. J., & Singer, W. (2013). High-frequency oscillations and the neurobiology of schizophrenia. *Dialogues in Clinical Neuroscience, 15*(3), 301–313.

McCutcheon, R. A., Reis Marques, T., & Howes, O. D. (2019). Schizophrenia—An overview. *JAMA Psychiatry, 77*(2), 201–210.

Reynolds, G. P., Abdul-Monim, Z., Neill, J. C., & Zhang, Z. J. (2004). Calcium binding protein markers of GABA deficits in schizophrenia—Postmortem studies and animal models. *Neurotoxicity Research, 6*(1), 57–61.

Deutsch, S. I., Rosse, R. B., Schwartz, B. L., Mastropaolo, J., Burket, J. A., & Weizman, A. (2010). Regulation of intermittent oscillatory activity of

pyramidal cell neurons by GABA inhibitory interneurons is impaired in schizophrenia: Rationale for pharmacotherapeutic GABAergic interventions. *Israel Journal of Psychiatry and Related Sciences*, 47(1), 17–26.

Gonzalez-Burgos, G., Cho, R. Y., & Lewis, D. A. (2015). Alterations in cortical network oscillations and parvalbumin neurons in schizophrenia. *Biological Psychiatry*, 77(12), 1031–1040.

Rujescu, D., Bender, A., Keck, M., Hartmann, A. M., Ohl, F., Raeder, H., Giegling, I., Genius, J., McCarley, R. W., Möller, H. - J., & Grunze, H. (2006). A pharmacological model for psychosis based on N-methyl-D-aspartate receptor hypofunction: Molecular, cellular, functional and behavioral abnormalities. *Biological Psychiatry*, 59(8), 721–729.

Coyle, J. T., Basu, A., Benneyworth, M., Balu, D., & Konopaske, G. (2012). Glutamatergic synaptic dysregulation in schizophrenia: Therapeutic implications. In Geyer, M. & Gross, G. (Eds.), *Novel antischizophrenia treatments* (Vol. 213, pp. 267–295). Springer.

Nair, P. C., McKinnon, R. A., Miners, J. O., & Bastiampillai, T. (2020). Binding of clozapine to the GABAB receptor: Clinical and structural insights. *Molecular Psychiatry*, 25(9), 1910–1919.

O'Donnell, B. F., Vohs, J. L., Krishnan, G. P., Rass, O., Hetrick, W. P., & Morzorati, S. L. (2013). The auditory steady-state response (ASSR): A translational biomarker for schizophrenia. *Supplements to Clinical Neurophysiology*, 62, 101–112.

Onitsuka, T., Oribe, N., & Kanba, S. (2013). Neurophysiological findings in patients with bipolar disorder. *Supplements to Clinical Neurophysiology*, 62, 197–206.

Brenner, C. A., Krishnan, G. P., Vohs, J. L., Ahn, W. Y., Hetrick, W. P., Morzorati, S. L., & O'Donnell, B. F. (2009). Steady state responses: Electrophysiological assessment of sensory function in schizophrenia. *Schizophrenia Bulletin*, 35(6), 1065–1077.

Lewis, D. A., Curley, A. A., Glausier, J. R., & Volk, D. W. (2012). Cortical parvalbumin interneurons and cognitive dysfunction in schizophrenia. *Trends in Neuroscience (Tins)*, 35(1), 57–67.

Newson, J. J., & Thiagarajan, T. C. (2018). EEG frequency bands in psychiatric disorders: A review of resting state studies. *Frontiers in Human Neuroscience*, 12, 521.

Reilly, T. J., Nottage, J. F., Studerus, E., Rutigliano, G., Micheli, A. I., Fusar-Poli, P., & McGuire, P. (2018). Gamma band oscillations in the early phase of psychosis: A systematic review. *Neuroscience and Biobehavioral Reviews*, 90, 381–399.

Lavoie, S., Polari, A. R., Goldstone, S., Nelson, B., & McGorry, P. D. (2019). Staging model in psychiatry: Review of the evolution of electroencephalography abnormalities in major psychiatric disorders. *Early Interv Psychiatry*, 13(6), 1319–1328.

Whitham, E. M., Pope, K. J., Fitzgibbon, S. P., Lewis, T., Clark, C. R., Loveless, S., Broberg, M., Wallace, A., DeLosAngeles, D., Lillie, P., Hardy, A., Fronsko, R., Pulbrook, A., & Willoughby, J. O. (2007). Scalp electrical recording during paralysis: Quantitative evidence that EEG frequencies above 20 Hz are contaminated by EMG. *Clinical neurophysiology: official journal of the International Federation of Clinical Neurophysiology*, 118(8), 1877–1888.

Whitham, E. M., Lewis, T., Pope, K. J., Fitzgibbon, S. P., Clark, C. R., Loveless, S., DeLosAngeles, D., Wallace, A. K., Broberg, M., & Willoughby, J. O. (2008). Thinking activates EMG in scalp electrical recordings. *Clinical neurophysiology: official journal of the International Federation of Clinical Neurophysiology*, 119(5), 1166–1175.

Pope, K. J., Fitzgibbon, S. P., Lewis, T. W., Whitham, E. M., & Willoughby, J. O. (2009). Relation of gamma oscillations in scalp recordings to muscular activity. *Brain Topography*, 22(1), 13–17.

Dharmaprani, D., Nguyen, H. K., Lewis, T. W., DeLosAngeles, D., Willoughby, J. O., & Pope, K. J., editors (2016). *A comparison of independent component analysis algorithms and measures to discriminate between EEG and artifact components*. 2016 38th Annual International Conference of the IEEE Engineering in Medicine and Biology Society (EMBC).

Fitzgibbon, S. P., DeLosAngeles, D., Lewis, T. W., Powers, D. M., Grummett, T. S., Whitham, E. M., Ward, L. M., Willoughby, J. O., & Pope, K. J. (2016). Automatic determination of EMG-contaminated compo-

nents and validation of independent component analysis using EEG during pharmacologic paralysis. *Clinical neurophysiology: official journal of the International Federation of Clinical Neurophysiology*, 127(3), 1781–1793.

Fitzgibbon, S. P., DeLosAngeles, D., Lewis, T. W., Powers, D. W. M., Whitham, E. M., Willoughby, J. O., & Pope, K. J. (2015). Surface Laplacian of scalp electrical signals and independent component analysis resolve EMG contamination of electroencephalogram. *International Journal of Psychophysiology*, 97(3), 277–284.

Fitzgibbon, S. P., Lewis, T. W., Powers, D. M. W., Whitham, E. M., Willoughby, J. O., & Pope, K. J. (2013). Surface Laplacian of central scalp electrical signals is insensitive to muscle contamination. *IEEE Transactions on Biomedical Engineering*, 60(1), 4–9.

Janani, A. S., Grummett, T. S., Lewis, T. W., Fitzgibbon, S. P., Whitham, E. M., DelosAngeles, D., Bakhshayesh, H., Willoughby, J. O., & Pope, K. J. (2017). Evaluation of a minimum-norm based beamforming technique, sLORETA, for reducing tonic muscle contamination of EEG at sensor level. *Journal of Neuroscience Methods*, 288, 17–28.

Janani, A. S., Grummett, T. S., Lewis, T. W., Fitzgibbon, S. P., Whitham, E. M., DelosAngeles, D., Bakhshayesh, H., Willoughby, J. O., & Pope, K. J. (2018). Improved artefact removal from EEG using Canonical Correlation Analysis and spectral slope. *Journal of Neuroscience Methods*, 298, 1–15.

Janani, A. S., Grummett, T. S., Bakhshayesh, H., Lewis, T. W., Willoughby, J. O., & Pope, K. J. (2018). *How many channels are enough? Evaluation of tonic cranial muscle artefact reduction using ICA with different numbers of EEG channels*. 26th European Signal Processing Conference (EUSIPCO).

Janani, A. S., Grummett, T. S., Bakhshayesh, H., Lewis, T. W., DeLosAngeles, D., Whitham, E. M., Willoughby, J. O., & Pope, K. J. (2020). Fast and effective removal of contamination from scalp electrical recordings. *Clinical neurophysiology: official journal of the International Federation of Clinical Neurophysiology*, 131(1), 6–24.

Delorme, A., Mullen, T., Kothe, C., Akalin Acar, Z., Bigdely-Shamlo, N., Vankov, A., & Makeig, S. (2011). EEGLAB, SIFT, NFT, BCILAB, and ERICA: New tools for advanced EEG processing. *Computational Intelligence and Neuroscience*, 2011, 130714.

Delorme, A., & Makeig, S. (2004). EEGLAB: An open source toolbox for analysis of single-trial EEG dynamics including independent component analysis. *Journal of Neuroscience Methods*, 134(1), 9–21.

Cardoso, J.-F. (1997). Infomax and maximum likelihood for blind source separation. *IEEE Signal processing letters*, 4(4), 112–114.

Goncharova, I. I., McFarland, D. J., Vaughan, T. M., & Wolpaw, J. R. (2003). EMG contamination of EEG: Spectral and topographical characteristics. *Clinical Neurophysiology*, 114(9), 1580–1593.

De Clercq, W., Vergult, A., Vanrumste, B., Van Paesschen, W., & Van Huffel, S. (2006). Canonical correlation analysis applied to remove muscle artifacts from the electroencephalogram. *IEEE transactions on Biomedical Engineering*, 53(12), 2583–2587.

Kayser, J., & Tenke, C. E. (2015). On the benefits of using surface Laplacian (current source density) methodology in electrophysiology. *International Journal of Psychophysiology*, 97(3), 171–173.

Perrin, F., Pernier, J., Bertrand, O., & Echallier, J. F. (1989). Spherical splines for scalp potential and current density mapping. *Electroencephalography and Clinical Neurophysiology*, 72(2), 184–187.

Willoughby, J. O., Fitzgibbon, S. P., Pope, K. J., Mackenzie, L., Medvedev, A. V., Clark, C. R., Davey, M. P., & Wilcox, R. A. (2003). Persistent abnormality detected in the non-ictal electroencephalogram in primary generalised epilepsy. *Journal of Neurology, Neurosurgery, and Psychiatry*, 74(1), 51–55.

Willoughby, J. O., Fitzgibbon, S. P., Pope, K. J., Mackenzie, L., & Davey, M., Wilcox, R. A., & Clark, C. R. (2003). Mental tasks induce gamma EEG with reduced responsiveness in primary generalized epilepsies. *Epilepsia*, 44(11), 1406–1412.

Fitzgibbon, S. P., Pope, K. J., Mackenzie, L., Clark, C. R., & Willoughby, J. O. (2004). Cognitive tasks augment gamma EEG power. *Clinical neu-

rophysiology: official journal of the International Federation of Clinical Neurophysiology, 115(8), 1802–1809.

Koka, K., & Besio, W. G. (2007). Improvement of spatial selectivity and decrease of mutual information of tri-polar concentric ring electrodes. Journal of Neuroscience Methods, 165(2), 216–222.

Uriguen, J. A., & Garcia-Zapirain, B. (2015). EEG artifact removal-state-of-the-art and guidelines. Journal of neural engineering, 12(3), 031001.

Tamminga, C. A., Pearlson, G. D., Stan, A. D., Gibbons, R. D., Padmanabhan, J., Keshavan, M., & Clementz, B. A. (2017). Strategies for advancing disease definition using biomarkers and genetics: The bipolar and schizophrenia network for intermediate phenotypes. Biological Psychiatry Cognitive Neuroscience Neuroimaging, 2(1), 20–27.

APPENDIX

FIGURE A1 Contamination graphs for Laplacians for all 115 electrodes and the three pruning methods, to supplement information in Figure 2. The contamination scale is shown in three corners of the figure and applies to all graphs.